

HOSTED BY



ELSEVIER

Contents lists available at ScienceDirect

Journal of Sustainable Mining

journal homepage: [www.elsevier.com/locate/jsm](http://www.elsevier.com/locate/jsm)

Research paper

## The presence and dosimetry of radon and thoron in a historical, underground metalliferous mine



Ross Kleinschmidt<sup>a,\*</sup>, Drew Watson<sup>a</sup>, Miroslaw Janik<sup>b</sup>, Gavin Gillmore<sup>c</sup>

<sup>a</sup> Radiation and Nuclear Sciences, Health Support Queensland, Queensland Department of Health, PO Box 594, Archerfield, Queensland, 4108, Australia

<sup>b</sup> National Institutes for Quantum and Radiological Science and Technology, 4-9-1 Anagawa, Inage-ku, Chiba-shi, 263-8555, Japan

<sup>c</sup> Department of Geography and Geology, School of the Natural and Built Environment, Faculty of Science, Engineering and Computing, Kingston University, Kingston-upon-Thames, Penrhyn Road, KT1 2EE, UK

### ARTICLE INFO

#### Keywords:

Radon  
Thoron  
Progeny  
Mines  
Dose  
NORM

### ABSTRACT

A combination of long term passive, and short term active radon-222, radon-220 and respective progeny measurements were conducted in both traverse and longitudinal axes of a historical metalliferous underground mine in North Queensland, Australia. While the passive monitor results provided average radon and thoron air concentrations over periods of 70–90 days, active measurements over a four day period provided significantly more detail into the dynamics of radon and progeny concentrations in the naturally ventilated mine environment. Passive monitor concentrations for radon and thoron ranged between 60 and 390 Bq m<sup>-3</sup> (mean: 140 ± 55 Bq m<sup>-3</sup>) and 140 and 2600 Bq m<sup>-3</sup> (mean: 1070 ± 510 Bq m<sup>-3</sup>) respectively, with passive thoron progeny monitors providing a mean concentration of 9 ± 5 Bq m<sup>-3</sup>EEC. Active measurement mean concentrations for radon, thoron, radon progeny and thoron progeny in the centre of the mine drive were 130 ± 90 Bq m<sup>-3</sup>, 300 ± 100 Bq m<sup>-3</sup>, 20 ± 20 Bq m<sup>-3</sup>EEC and 10 ± 10 Bq m<sup>-3</sup>EEC respectively.

It was identified that thoron passive detector placement is critical in establishing reliable monitoring data, and is the reason for the discrepancy between the active and passive thoron results in this study. Site specific progeny measurements are required for the accurate estimation of dose to persons entering the mine. Based on short term active measurements and passive thoron progeny monitor results, the dose contribution from thoron and progeny in the mine was observed to contribute up to 80% of the total radon/thoron inhalation dose, and therefore should not be underestimated in monitoring programs under similar conditions.

## 1. Introduction

### 1.1. Underground mines and radon

As the resource sector extends its exploration activities, many historical and currently abandoned mines are being re-evaluated for mining potential. Assessment of mineral resources in these mines generally requires geophysicists and geologists be given access to them in order to explore. Other parties that may enter mines of this nature consist of caving enthusiasts, mining history societies, industrial archaeologists, mineral specimen collectors, tourists, and fauna conservation officers.

Radon-222 (radon, half-life: 3.8 days) and radon-220 (thoron, half-life: ~55 s), both inert radioactive gases, are considered to be Naturally Occurring Radioactive Materials (NORM) that are formed in the decay

series of uranium-238 and thorium-232, respectively. Both radon and thoron radioisotopes decay to their respective radioactive progeny due to the emission of alpha & beta particles and gamma radiation, and these progeny radionuclides largely determine the dose delivered upon inhalation. Radon isotopes may enter underground environments such as mines in a number of ways, including emanation from host rock and dissolution from mine/ground waters. External radiation exposure from primordial radioactive elements such as uranium and thorium, which are also NORM, may be an additional contributing factor to the level of an individual's dose.

There is considerable evidence to show that excessive radon levels in underground mines causes lung cancer in miners, as highlighted by Muirhead et al. (1993). Various other health effects of radon exposure have also been revealed on the basis of epidemiological studies, including skin cancer (Wheeler, Allen, Depledge, & Curnow, 2012) and

\* Corresponding author.

E-mail address: [ross.kleinschmidt@health.qld.gov.au](mailto:ross.kleinschmidt@health.qld.gov.au) (R. Kleinschmidt).

<https://doi.org/10.1016/j.jsm.2018.06.003>

Received 16 March 2018; Received in revised form 22 April 2018; Accepted 7 June 2018

Available online 15 June 2018

2300-3960/ © 2018 Published by Elsevier B.V. on behalf of Central Mining Institute. This is an open access article under the CC BY-NC-ND license (<http://creativecommons.org/licenses/by-nc-nd/4.0/>).

leukaemia (Cogliano et al., 2011). Studies by Lubin and Boice (1997), and Darby et al. (1998) have produced convincing evidence that radon is a health hazard. The International Commission on Radiological Protection (ICRP), and more recently the World Health Organisation, have concluded that excessive radon levels are a health hazard (ICRP, 2010; ICRP, 2014; WHO, 2009; WHO, 2018).

Radon and radon progeny interrelationships and characteristics in underground mines, caves and indoor environments are reasonably well understood and numerous pieces of work have been published (Gillmore, Sperrin, Phillips, & Denman, 2000a, 2000b; Dixon, 1996; Gillmore, Gharib, Denman, Phillips, & Bridge, 2011; Gillmore, Phillips, Denman, Sperrin, & Pearce, 2001; Miles et al., 2007; Mudd, 2008; Przylibski, 2001; Stojanovska et al., 2014). UNSCEAR (2017), however, claim that more studies for both radon and thoron are required and have started a systematic review of literature and published data available for thoron and progeny assessments, including measurement techniques and thoron equilibrium factor determinations (e.g. Chen, Moir, Sorimachi, Janik, & Tokonami, 2012; Janik et al., 2013; Khater, Hussein, & Hussein., 2004; Kávási et al., 2007; McLaughlin et al., 2011; Nuccetelli & Bochicchio, 1998; Solli, Anderson, Stranden, & Langård, 1985). It has more recently been identified that thoron may be a significant contributor to inhalation dose as measured for indoor air (Chen et al., 2012; Misdaq & Ouguidi, 2011; Ningappa, Sannappa, Chandrashekar, & Paramesh, 2009; Yamada et al., 2006), and it is reasonable to assume that this would also apply to the underground mine environment.

There is a lack of publicly available information on radon, thoron and respective progeny concentrations and external exposure levels in historical mines. Assessment of environmental and human health impact needs to be considered for these environments.

## 1.2. Mine location and history

The study mine is located at Bamford Hill, approximately 95 km WSW from the town of Cairns on the North Queensland east coast, Australia (Fig. 1). Between 1893 and 1906 wolframite (tungsten) was mined from eluvial and alluvial deposits in the Bamford area, eventually this led to hard rock extraction of wolframite, molybdenite and bismuth from quartz pipes. A stamp battery was commissioned by the government to service the local mines in 1917 and operated sporadically until 1949. From the late 1970s, and fluctuating with market demand, underground mining and exploration continued in the Bamford Hill area up until the 1980s (Blevin, 1989).

The exploration mine is a simple horizontal adit cut into the base of Bamford Hill, approximately 330 m long with a number of shorter crosscuts and at least one confirmed chimney (rise 2, Fig. 1). It is located in a remote location and has no electricity, fixed lighting or means of securing access to the portal. The mine is naturally ventilated, based on differing air pressures associated with a difference in elevation (height above sea level) between openings to the atmosphere, the adit portal and the chimney at the end of the adit. External, seasonal temperatures influence the air flow velocity and direction within the mine.

The mine was mapped for this project by Wolfram Camp Mining geologists using a GeoSLAM ZEB1<sup>®</sup> handheld 3D laser profiler, providing a 3D point cloud, wireframe and rendered map of the adit, surface area and volume data (Fig. 1), and additionally, a video “fly through” of the mine to visualise the structure and characteristics.

The local environment is subtropical with a characteristic wet season in summer (temperature range: 21–31 °C, RH: 67%, rainfall: 554 mm) influenced by the fringe effects of monsoonal and cyclonic weather patterns typical for coastal regions in northern Australia. Winters are typically dry and relatively cool (temperature range: 26 to 12 °C, RH: 64%, rainfall: 29 mm). The annual evaporation is 2000 mm and winds are predominantly north-east/east/south east (BOM, 2018).

## 1.3. Geology

The test mine intersects the Bamford Hill tungsten-molybdenum-bismuth deposits hosted within the Carboniferous Bamford Granite intrusions of the local Featherbed Caldera complex. The granite contains quartz, feldspars, minor Fe-Al rich biotite and minor allanite, magnetite, xenotime and zircon – the latter being likely sources for the radioactive elements uranium and thorium. Wolframite and molybdenite are deposited within quartz rich pipe-like bodies and greisen within the granite (Blevin, 1989).

Within the test mine, porphyric volcanics extend for approximately 30–40 m from the drive portal. Beyond that, the drive intersects a mix of variably altered granite and greisen, the latter being more intensely developed adjacent to the quartz-Mo-W (ore) pipes.

## 2. Method

### 2.1. Sampling methods and location

Monitor packages in campaigns 1 and 2 were both deployed both down the length of the main adit, in proximity to the mine wall surfaces as described in Table 1 and shown in Fig. 5 (i.e. monitor package distance from portal). A number of passive monitor types were utilised during the project for comparison and quality purposes.

The packages were suspended from the wall surface using existing blast drill holes as mounting points at wall to package distances of between 5 mm and 250 mm. The availability of convenient holes and wall surface roughness restricted the ability to precisely place each package; this is taken into consideration in the interpretation of results.

Campaign 3 was undertaken to more closely examine spatial and short term temporal radon and thoron characteristics across cross sections of the mine. Passive monitor packages in campaign 3 were mounted on a suspended chain at approximately 1500 mm above the mine's ground surface, with two active instruments placed at cross section A-A', one at the centre of the cross section, and one in proximity to the mine wall.

Rock specimens were collected throughout the mine to establish natural radioactivity levels in the immediate environment. Hand sized specimens were collected from the locations shown in Fig. 1, for high resolution gamma ray spectrometry and elemental analysis.

#### 2.1.1. Gamma spectrometry

Rock samples were analysed using high resolution gamma ray spectrometry (HRGS) and were crushed and pulverised to pass through a 200 µm sieve. The pulverised material was packed into 80 mL aluminium cans sealed with a NITON<sup>®</sup> gasket for a minimum period of 20 days prior to counting in order to allow the ingrowth of uranium and thorium progeny. Gamma-ray spectrometers (EG&G Gamma-X detectors, 35–45% rel. efficiency) were calibrated using IAEA RGU-1, IAEA RTh-1 and IAEA RGK-1 reference materials (IAEA, 1987) prepared to have the same geometry as the samples. Typical counting times were between 20 h and 48 h. The HRGS analysis suite included U-238 (via Th-234), Ra-226 (via Pb/Bi-214), Th-232 (via Ac-228, Pb/Bi-212 and Tl-208), and K-40.

#### 2.2. Passive monitors

A number of passive radon, thoron, thoron progeny and gamma monitors were used over 3 monitoring campaigns. Table 1 provides details of the monitors used, monitoring periods and placement data. All passive monitors were used with a protective hood over the top of the packages to minimise the impact of environmental contamination from dripping water, dust deposition and wildlife interference (Fig. 2 and Fig. 3).

The RADUET<sup>®</sup> monitors were purchased from and analysed by RADOSYS Kft. The monitor consists of two CR-39 (polyallyl diglycol

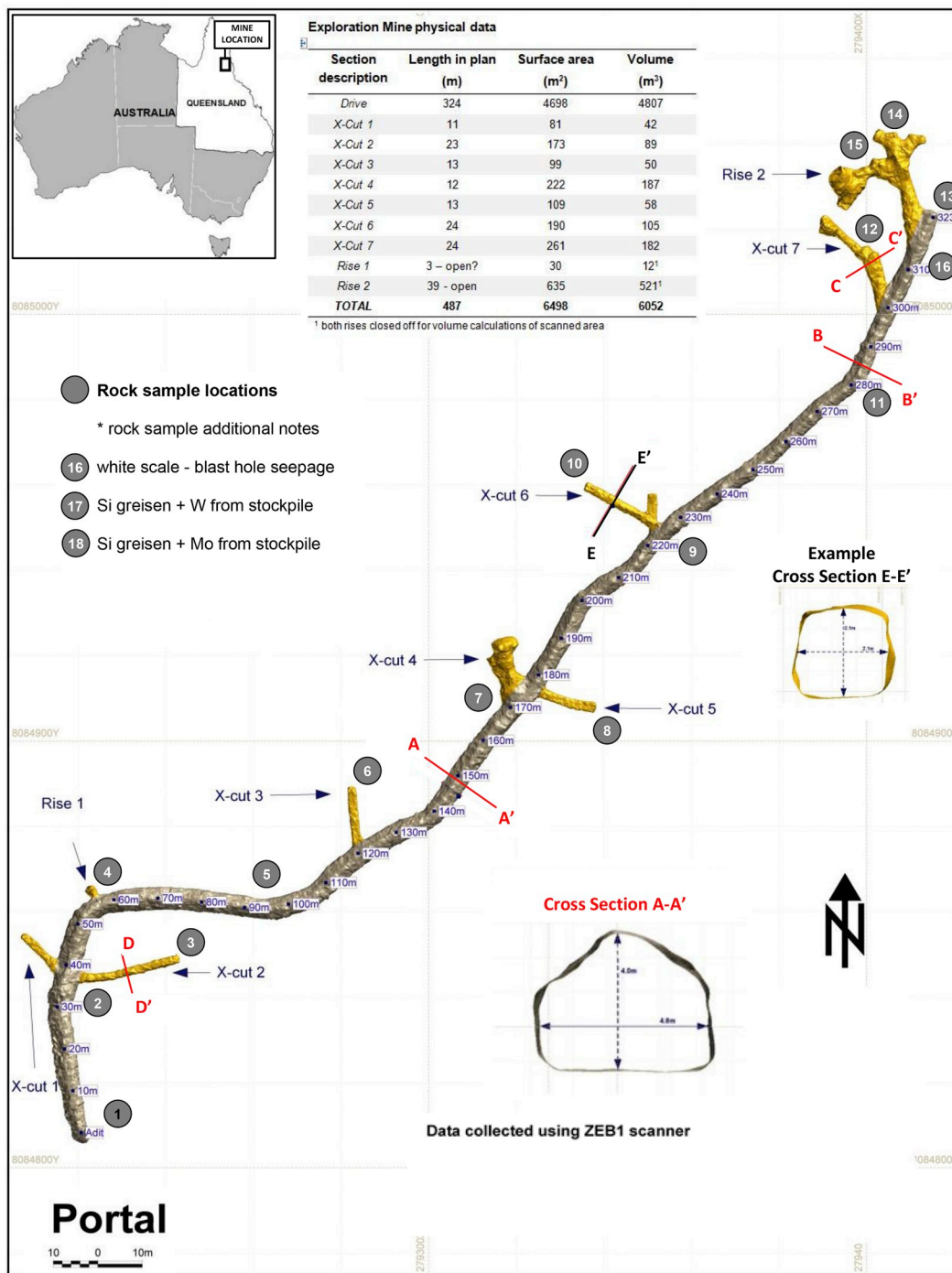


Fig. 1. Bamford Hill mine location, mapping and sampling sites.

carbonate or PADC) plastic detectors, one mounted in slow diffusion rate housing, the other in fast diffusion housing, to allow discrimination between radon and thoron (Zhuo, Iida, Moriizumi, Aoyagi, & Takahashi, 2001; Tokonami, Takahashi, Kobayashi, Zhuo, & Hulber, 2005). The RADUET monitors were used as the primary monitors for the 2015 program (campaign 1 and 2) and as quality monitors for campaign 3. Duplicate RADUET monitors were deployed in a number of locations, representing approximately 5% of all the monitors used.

The RSKS<sup>®</sup> monitors are of RADOSYS Kft design and were supplied and analysed by Kingston University, the United Kingdom. The monitor consists of a single PADC CR-39 plastic detector placed inside a slow diffusion chamber for the measurement of radon only. The RSKS

monitors were used in the 2015 campaign 1 program for comparison/quality purposes.

TASL<sup>®</sup> radon and thoron monitors were supplied, processed and read by Radiation and Nuclear Sciences (RNS). The monitors are comprised of a PADC CR-39 plastic chip in slow diffusion housing for radon and fast diffusion housing to allow thoron measurement.

Passive gamma monitors are supplied and analysed by the Australian Radiation Protection and Nuclear Safety Agency (ARPANSA). The monitors utilise thermoluminescent detectors (TLD) using CaSO<sub>4</sub>:Dy chips, and are corrected for environmental radiation gamma energy response. Results are provided in units of nanoGray per hour. The TLD monitors were used in campaigns 1 and 2.

**Table 1**  
Monitoring periods, detectors and sampling locations.

Period	Detector	Measurand	Location
<b>Campaign 1</b> 10 Jun 2015 to 10 Sep 2015 (92 days) Season – WINTER	RADUET® ARPANSA CaSO <sub>4</sub> :Dy TLD EXTECH® RHT50 datalogger Kingston UK RSFS®	radon, thoron (Bq m <sup>-3</sup> ) gamma (nGy h <sup>-1</sup> )  humidity (%RH), temp (°C), pressure (mbar) radon (Bq m <sup>-3</sup> )	All monitors mounted between 5 and 250 mm from the wall surface. Refer to supplementary data for spatial distribution of all monitors.
<b>Campaign 2</b> 10 Sep 2015 to 10 Dec 2015 (91 days) Season – SPRING	RADUET® ARPANSA CaSO <sub>4</sub> :Dy TLD EXTECH® RHT50 datalogger	radon, thoron (Bq m <sup>-3</sup> ) gamma (nGy h <sup>-1</sup> )  humidity (%RH), temp (°C), pressure (mbar)	All monitors mounted between 5 and 250 mm from the wall surface. Refer to supplementary data for spatial distribution of all monitors.
<b>Campaign 3a</b> 09 Aug 2016 to 19 Oct 2016 (71 days) Season – WINTER/SPRING	RADUET® RNS TASL® Rn/Tn NIRS TnP  EXTECH® RHT50 datalogger	radon, thoron (Bq m <sup>-3</sup> ) radon, thoron (Bq m <sup>-3</sup> ) Thoron progeny (Bq m <sup>-3</sup> EEC) humidity (%RH), temp (°C), pressure (mbar)	every 250 mm across transects A-A', B-B', C-C' and D-D' at 1500 mm above ground surface
<b>Campaign 3b</b> 08 Aug 2016 to 11 Aug 2016 (4 days) Season – WINTER	SARAD EQF3200  Testo 4352 + hotwire anemometer (0635-1025)	radon, thoron + respective progeny (Bq m <sup>-3</sup> /Bq m <sup>-3</sup> EEC)  Air velocity (ms <sup>-1</sup> ), temp (°C)	“centre”, s/n: 00167, centre of section A-A' “wall”, s/n 00168, 300 mm from side wall, section A-A' (2 h sampling period) mounted on EQF3200 s/n 167 (1 h sampling period)

Passive thoron progeny monitors used in the 2016 campaign, at locations A-A', B-B', C-C' and D-D' (Fig. 1), were developed and supplied by the Japanese National Institute of Radiological Sciences (NIRS) based on the design proposed by Zhuo, Iida and Hashiquchi (2000) and Zhuo, Tokonami, Yonehara, and Yamada (2002), using one PADCR CR-39 chip covered with thin sheets of absorbers. The modified version of thoron progeny monitor (TnP monitor) by NIRS (Fig. 4), applied to this survey, consists of two 1 × 1 cm PADCR CR-39 chips covered with an aluminium-vaporized Mylar film of 71 mm air-equivalent thickness and polypropylene film. The thickness of absorbers was adjusted to only allow 8.78 MeV  $\alpha$ -particles emitted from <sup>212</sup>Pb reach the detector. The use of two chips provides better statistics and lower measurement uncertainty. Based on an NIRS laboratory calibration, the airborne concentration of the thoron decay product <sup>212</sup>Pb in the air is determined and can be expressed as Bq m<sup>-3</sup> EETC. The NIRS monitors have been used and proven in other large-scale surveys (Janik et al., 2013; McLaughlin et al., 2011; Omori et al., 2016; Ramola et al., 2012).

Background measurements from non-exposed monitors were

subtracted from total counts of exposed monitors. Additionally, for each series of CR-39 chips a new calibration factor was determined using NIRS radon and thoron chambers. The thoron progeny monitors were additionally tested in the thoron experimental house constructed in Helmholtz Zentrum Munchen (HMGU) (Tschiersch & Meisenberg, 2010), Germany and in the thoron exposure chamber of Hiroasaki University, Japan. TnP monitors were deployed in pairs to further increase the reliability of results.

### 2.3. Active measuring instruments

Radon, thoron and their respective progeny were measured during the 2016 campaign (campaign 3b) at cross section A-A' (Fig. 1) using SARAD® EQF3200 instruments sampling over 120 min periods for approximately 4 days. One tripod mounted instrument (at 1500 mm above ground) was deployed with its air intake 300 mm from the mine wall surface and the second instrument in the centre of the drive, approximately 2500 mm from the mine wall surface. Instrument air intakes



Fig. 2. Example of monitor sampling packages for 2015 monitoring campaigns.

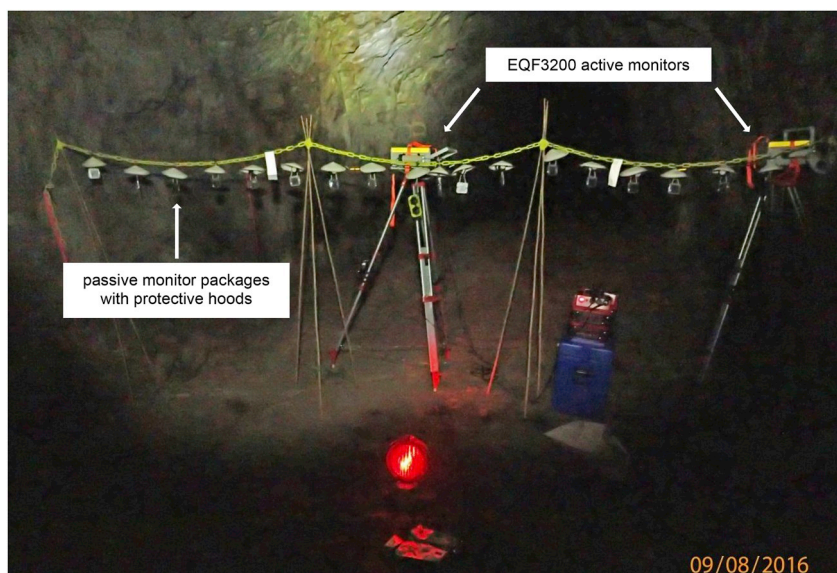


Fig. 3. Example of monitor sampling packages for the 2016 monitoring campaign and the location of EQF3200 active monitoring instruments at section A-A' (Fig. 1).

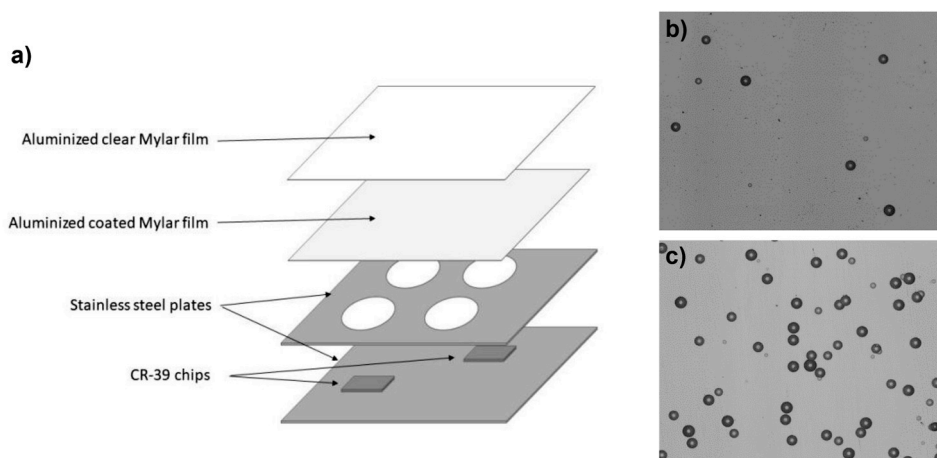


Fig. 4. a) Schematic view of TnP monitor modified by NIRS (reproduced from Janik et al., 2013); example scan of etched CR-39 from, b) calibration, and c) exposure in mine.

were placed perpendicular to the longitudinal axis of the drive to minimise the effects of air movement direction through the mine. In addition to radon isotopes and progeny, each instrument records temperature, air pressure and relative humidity for each period.

A hot wire anemometer (Testo<sup>®</sup> 4352 + hotwire anemometer Model No. 0635-1025) was attached to each instrument to measure air velocity, with results recorded every 60 min. External power was supplied to the instruments using two portable 12 v, 48 Ah batteries (Fig. 3).

Additional temperature, air pressure and relative humidity data was collected using EXTECH<sup>®</sup> RHT50 dataloggers mounted with passive radon/thoron monitors, operating on a 60 min measurement cycle (Table 1).

#### 2.4. Quality

A range of passive radon or radon/thoron monitors were used throughout the project depending on their availability and, additionally, duplicate monitors were deployed for quality purposes. The quality monitoring methods for the passive monitors included the use of:

- Duplicate RADUET monitors, campaign 1 and 2,

- Comparative RSKS monitors from Kingston University in campaign 1,
- Comparative RADUET monitors in campaign 3.

Active radon, thoron and their respective progeny instruments were calibrated by the manufacturer and compared with reference instruments in the ARPANSA radon chamber.

### 3. Results and discussion

#### 3.1. Host geology and NORM

HRGS results for collected rock specimens are given in Table 2. The majority of specimens were of the host granite complex with minor mineralised areas producing higher uranium and thorium concentrations. Porphyric volcanics typically were observed to have lower uranium and thorium concentrations. Mean activity concentrations were tabled and the terrestrial derived air kerma rate estimated for a 4 $\pi$  geometry, using conversion factors adapted from Malins, Machida, and Saito (2015). Assuming the rock specimens are representative of the material comprising the internal surfaces of the mine, a mean derived air kerma rate of  $360 \pm 70$  nGy h<sup>-1</sup> can be compared with the

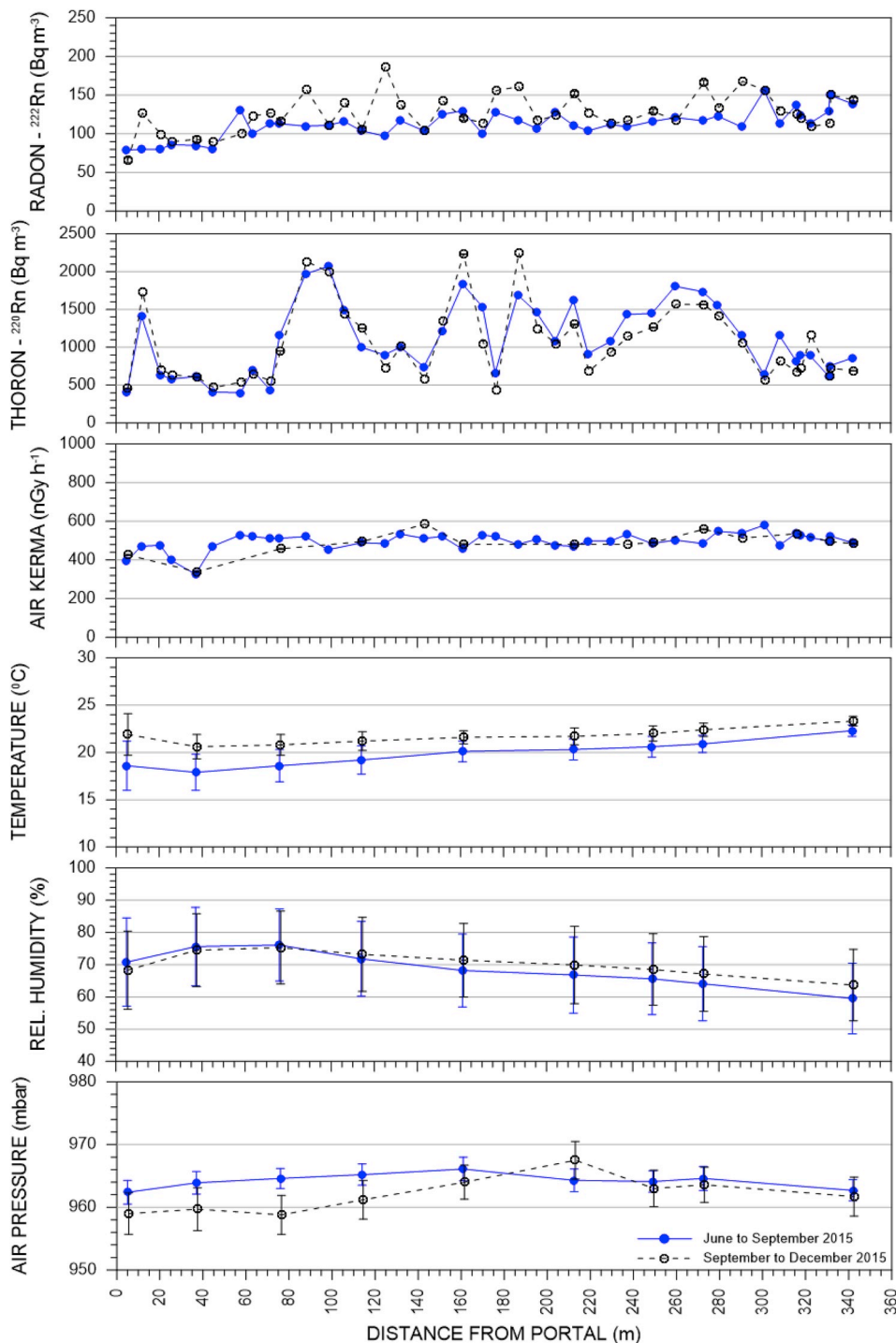


Fig. 5. Results from campaign 1 and 2 passive monitors and environmental data loggers.

geometric mean value for the gamma exposure rate determined from the passive TLD monitors (all campaigns) of  $490 \pm 140 \text{ nGy h}^{-1}$ , noting that the TLD data is not corrected for cosmic radiation contribution of up to  $56 \text{ nGy h}^{-1}$  (CARI-7 software, FAA, 2017).

### 3.2. Campaign 1 and 2

A summary of results for passive radon, thoron and gamma monitors, and environmental data loggers is given in Fig. 5. The environmental data suggests that diurnal temperature variation reduces towards the end of the mine to a constant 23 °C, irrespective of seasonal

variation (June to September – Winter, vs September to December (Spring)). Relative humidity decreases towards the end of the mine, however variation remains consistent with the variation at the portal.

Air kerma (gamma) results were observed to be constant across both monitoring campaigns. The decreased air kerma rate from the portal to approximately 30 m is considered to be associated with the geology change from porphyric volcanics to granite as noted in Section 1.3, and is supported by gamma spectrometry results provided in Table 2.

The radon results show minimal variation in the radon concentration between the portal and the end of the mine. There is negligible variation between sampling periods from campaign 1 and 2. It is

**Table 2**  
Gamma spectrometry results for rock samples collected from the mine (refer Fig. 1).

Sample ID	Activity concentration (Bq kg <sup>-1</sup> )			
	U-238 <sup>a</sup>	Ra-226 <sup>a</sup>	Th-232 <sup>a</sup>	K-40
1	120 ± 30	87 ± 3	130 ± 10	1440 ± 100
2	70 ± 10	44 ± 2	78 ± 7	1370 ± 120
3	160 ± 20	111 ± 4	121 ± 9	1360 ± 100
4	720 ± 60	240 ± 20	150 ± 10	40 ± 10
5	200 ± 30	103 ± 6	110 ± 10	1560 ± 110
6	180 ± 20	128 ± 9	120 ± 10	880 ± 80
7	180 ± 20	176 ± 9	140 ± 10	1410 ± 100
8	240 ± 20	150 ± 10	130 ± 10	150 ± 10
9	170 ± 20	118 ± 8	120 ± 10	1360 ± 120
10	150 ± 20	86 ± 5	140 ± 10	1310 ± 100
11	210 ± 20	210 ± 10	140 ± 10	1180 ± 90
12	140 ± 30	113 ± 6	96 ± 7	310 ± 30
13	210 ± 30	149 ± 8	180 ± 20	520 ± 50
14	240 ± 30	240 ± 10	240 ± 20	260 ± 20
15	90 ± 10	73 ± 4	107 ± 8	640 ± 50
16	30 ± 10	280 ± 20	20 ± 3	70 ± 10
17	200 ± 20	200 ± 10	180 ± 10	480 ± 40
18	130 ± 20	159 ± 9	160 ± 10	970 ± 70
<b>Mean<sup>b</sup></b>	<b>200 ± 50</b>	<b>140 ± 20</b>	<b>130 ± 20</b>	<b>920 ± 150</b>
<b>Derived air kerma rate<sup>c</sup> (nGy h<sup>-1</sup>), 4π</b>				<b>360 ± 70</b>

<sup>a</sup> Activity concentration determined from short half-life progeny radionuclides.

<sup>b</sup> Mean activity only includes Sample ID 1 to 15 (refer Fig. 1), uncertainty is 2σ (95%).

<sup>c</sup> Using mean activity concentration results and conversion factors (Malins et al., 2015) – corrected for 4π geometry (terrestrial only).

thought that marginally lower radon concentrations near the portal may be associated with both proximity to the open atmosphere and therefore increased air exchange, and reduced uranium concentration in the local host geology.

Thoron results vary considerably along the length of the mine, ranging from approximately 400 Bq m<sup>-3</sup> to 2300 Bq m<sup>-3</sup>. The concentrations at sampling locations showed the same trends for both campaign 1 (winter) and campaign 2 (spring); the same sampling location and sampling package mount was used for the respective campaigns.

The thoron data from campaign 1 and 2 is considered to be compromised due to the sampling packages containing the passive thoron monitors being placed at varying distances from the exhalation surface (wall) and therefore within zones of high thoron concentration variability. The impact of this irregular monitoring positioning can be seen in the data gathered in campaign 3, as shown in Fig. 6 and Fig. 7. The results highlight the need to establish an optimal sampling distance, fit for the project purpose, as thoron concentration varies significantly over distances up to 500 mm from the exhalation surface.

### 3.3. Campaign 3

#### 3.3.1. Passive monitors

Campaign 3a utilised passive monitors to measure radon, thoron and thoron progeny for several mine cross-sections in order to establish exhalation surface effects and compare passive results with shorter term active measurement systems. Fig. 6 shows results from the 71 day monitoring period, for cross-sections A through D (Fig. 1).

The results show that both radon and thoron progeny concentrations in air appear to be independent of proximity to the exhalation surfaces and therefore remain relatively constant across each section. Thoron concentration, however, varies significantly depending on the distance from the exhalation surface, becoming more stable in the centre of each cross-section. This effect is thought to be responsible for the greatly varying thoron results in campaign 1 and campaign 2.

Based on mean thoron monitor results (excluding measurement points less than 250 mm from the exhalation surface) and mean TnP results for each cross section, the mean thoron equilibrium factors (TnF<sub>eq</sub>) are 0.028 at section A-A'; 0.018 at section B-B'; 0.014 at section C-C'; and 0.011 at section D-D'. The calculated equilibrium factors compare favourably with those published by Chen et al. (2012).

The radon and thoron results for sections C-C' and D-D' are elevated when compared with those from sections A-A' and B-B', this observation may be related to a combination of marginally elevated concentration of uranium and thorium in the mineralised zones present in the cross cuts, and the reduced air flow within the respective volumes.

#### 3.3.2. Active monitors

Campaign 3b utilised 2 active instruments to measure radon, thoron and progeny at section A-A' (Fig. 1). Fig. 7 shows a composite plot of collected data over approximately 4 days. Air velocity data was also collected. The data gap in Fig. 7b relates to an instrument data recording failure for a short period during the measurement program. Air velocity data shows maximums of over 0.4 m s<sup>-1</sup> between 18:00 and 06:00 h (night time) at the centre of section A-A'. It should be noted that there is potential for some minor fauna related air movement within the mine due to the presence of a significant colony of up to several hundred bats, typically active at dawn and dusk, in addition to the movement generated through naturally pumped ventilation processes.

Averaged thoron concentrations at the wall and in the centre of section A-A' show the same trend as the passive monitor results for similar locations (Fig. 6), i.e. elevated thoron near the wall exhalation surface. Diurnal variations in radon, thoron and progeny concentrations are evident in both the wall and centre locations, although they are marginally out of phase between the monitoring locations.

It can be observed that thoron levels at the central monitoring location are at their lowest concentration at periods of low air movement. This can be attributed to the short half-life of thoron which results in it being unable to reach the central elevated monitoring location under still conditions before decay. When the air becomes mixed through air movement, the concentration at the exhalation surfaces is distributed more consistently throughout the mine.

Periodic relationships were also observed for progeny concentration and equilibrium factors. The section centre thoron equilibrium factors of up to 0.4, during low air velocity periods during each day, and radon and thoron concentration variations by a factor of 4 over diurnal periods are of interest.

#### 3.3.3. Dose estimation

For the purposes of dose estimation, it is assumed that the contribution from radon and thoron gas inhalation is negligible.

The total dose rate, DR<sub>T</sub>, in units of μSv h<sup>-1</sup>, is calculated using:

$$DR_T = DR_{iRn} + DR_{iTn} + DR_e \quad (1)$$

where the respective radon (DR<sub>iRn</sub>) and thoron (DR<sub>iTn</sub>) inhalation dose rates are calculated using:

$$DR_{iRn} = C_{Rn} \times Rn_{EqF} \times DCF_{Rn} \quad (2)$$

where C<sub>Rn</sub> is the mean radon concentration in Bq m<sup>-3</sup>, Rn<sub>EqF</sub> is the measured radon progeny equilibrium factor, and DCF<sub>Rn</sub> is the radon dose conversion factor of 1.3 · 10<sup>-5</sup> mSv/Bq h m<sup>-3</sup>EEC ("indoor workplace" – ICRP, 2017), and

$$DR_{iTn} = C_{Tn} \times Tn_{EqF} \times DCF_{Tn} \quad (3)$$

where C<sub>Tn</sub> is the mean radon concentration in Bq m<sup>-3</sup>, Tn<sub>EqF</sub> is the measured thoron progeny equilibrium factor, and DCF<sub>Tn</sub> is the radon dose conversion factor of 1.2 · 10<sup>-4</sup> mSv/Bq h m<sup>-3</sup>EEC ("indoor workplace" – ICRP, 2017), and

$$DR_e = E_\gamma \times CF_e \quad (4)$$

where E<sub>γ</sub> is the mean gamma air kerma rate in μGy h<sup>-1</sup>, and CF<sub>e</sub> is the

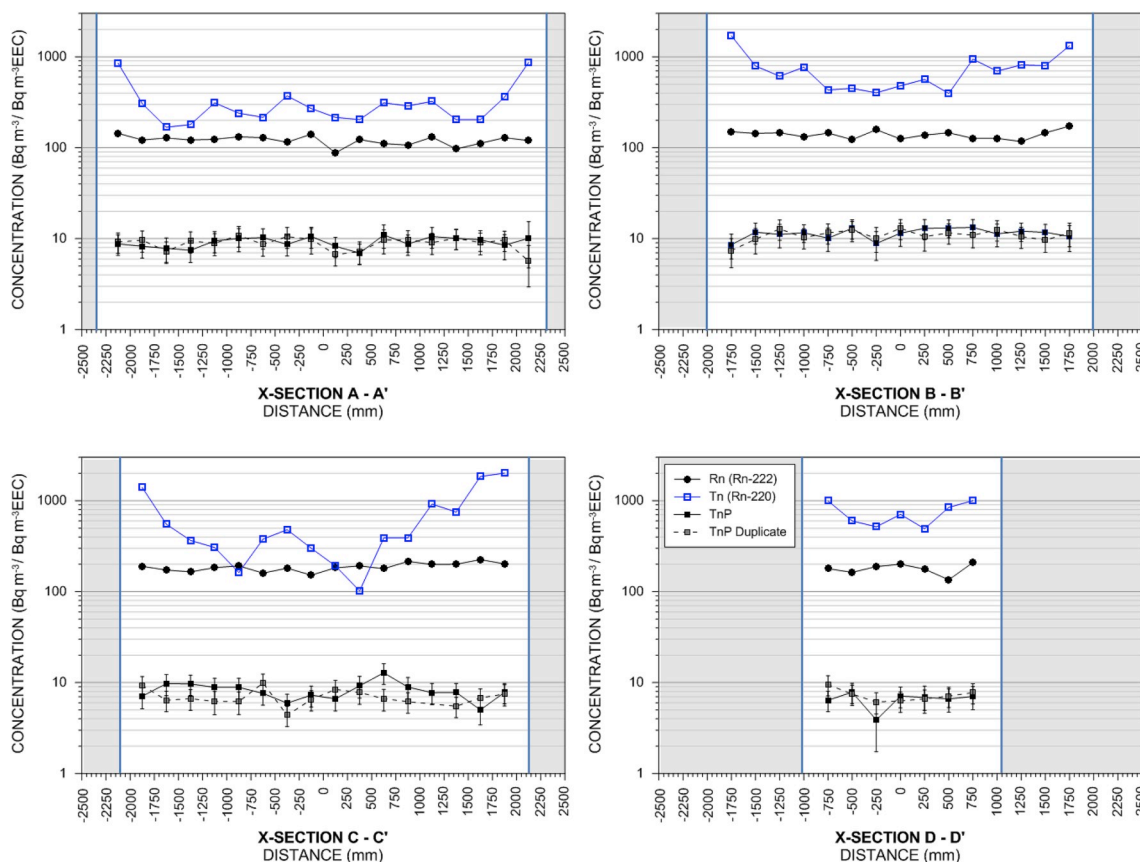


Fig. 6. Radon, thoron and thoron progeny concentrations from passive monitors, at cross sections A-A', B-B', C-C' and D-D' (Fig. 1).

air kerma to dose conversion factor of  $0.7 \text{ Sv Gy}^{-1}$  (UNSCEAR, 2006).

Alternatively,  $DR_{Rn}$  and  $DR_{Tn}$  can be calculated by directly using  $RnP$  and  $TnP$  data, multiplied by the respective dose conversion factors provided in equation (2) and equation (3). A summary of results from all campaigns and used in the dose calculations is provided in Table 3.

Thoron concentration values used for calculation purposes are based on results observed at distances greater than 500 mm from any exhalation surface. Table 3 shows mean (arithmetic) results useful for the comparison of data generated from passive and active monitoring programs, and the calculation of dose estimates using formulas 1 to 4 above. The dose rate associated with entering the mine, using the data provided and calculated as above, is given in Table 4.

### 3.3.4. Quality measurements

Duplicate RADUET monitors from campaign 1 and 2 showed good agreement for both radon and thoron results, within 20% and 25%, respectively.

The comparative RSKS monitors used in campaign 1 generally overestimated radon concentration by 30%, and in several cases by up to 110%, when compared to the RADUET monitors. It was observed that thoron concentrations were at the highest values where the RSKS monitors indicated a significant overestimation of radon concentration. It is thought that the RSKS monitors may be sensitive to thoron at these higher concentrations.

Campaign 3 TASL radon and thoron monitor results were compared with a number of RADUET monitors results. The percentage variation of the TASL to RADUET monitor results was less than 25% for both radon and thoron.

## 4. Conclusions

An assessment of radiation dose for persons entering a historical,

underground mine was conducted via the summation of inhalation and external dose components. The inhalation component included both radon and thoron related exposure pathways, based on mean results over several measurement campaigns. As it is considered that entry to the mine would be intermittent for the purposes previously outlined, the dose rate has been calculated in units of  $\mu\text{Sv h}^{-1}$ , allowing for simple total dose calculation based on hours of entry. Table 4 shows a calculated dose of approximately  $1.8 \mu\text{Sv h}^{-1}$  for a person entering the mine based on average results. If generic UNSCEAR (2006) equilibrium factors are used in conjunction with the mean radon and thoron concentration results from this study, the dose is estimated at  $2.46 \mu\text{Sv h}^{-1}$ .

Thoron contributes 81% of the inhalation dose based on the study results.

While there is good agreement between long term, integrating passive monitor results and mean results from shorter active measurement regimes, temporal factors only identified by the active measurements suggest that there is potential for a higher inhalation dose for persons entering the mine during different times of the day.

Radon and associated progeny concentrations appear to be relatively constant throughout the mine, only increasing in cross cut drives where air exchange rates are reduced.

If persons entering the mine are working in close proximity to the mine wall surfaces, there is potential for the inhalation of higher concentrations of thoron gas, however, the dose contribution associated with gas inhalation is negligible. Thoron progeny inhalation is of importance and was observed to remain relatively constant irrespective of distance from the exhalation surface.

A significant observation relates to sampling with respect to the positioning of passive thoron gas monitors. Thoron monitoring results from campaign 3 highlight the need to ensure monitors of this type are placed at an equal distance from any exhalation surface, and this distance should be determined depending on the purpose of the program



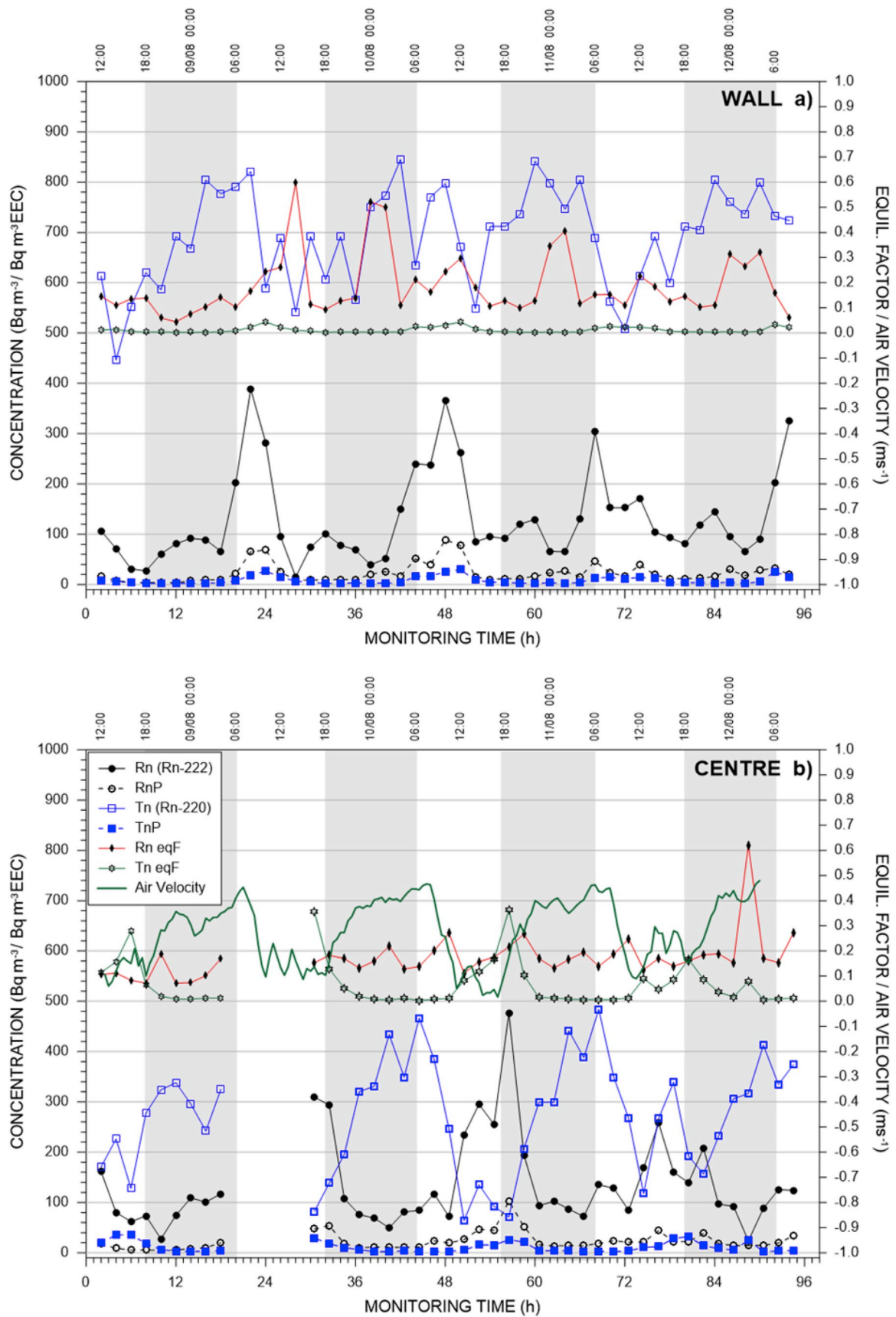


Fig. 7. Active measurement results for cross section A-A' (Fig. 1) at a) wall, and b) centre.

**Table 3**  
Summary data for all radon/thoron measurement campaigns (uncertainty is the standard deviation of multiple results).

Sampling campaign	$C_{Rn}$	$RnP$	$Rn_{EqF}$	$C_{Tn}$	$TnP$	$Tn_{EqF}$
	Bq m <sup>-3</sup>	Bq m <sup>-3</sup> EEC	Bq m <sup>-3</sup>	Bq m <sup>-3</sup>	Bq m <sup>-3</sup> EEC	Bq m <sup>-3</sup>
1	130 ± 60	–	–	960 ± 480	–	–
2	150 ± 60	–	–	930 ± 540	–	–
3a <sup>a</sup>	120 ± 30	–	–	330 ± 200	9 ± 3	0.028
3b (wall)	130 ± 90	20 ± 20	0.176	690 ± 100	8 ± 8	0.012
3b (centre)	140 ± 100	20 ± 20	0.167	270 ± 100	10 ± 10	0.040
Mean <sup>b</sup>	130	23	0.167	300	10	0.034
UNSCEAR <sup>c</sup>	–	–	0.400	–	–	0.040

<sup>a</sup> Value is the average of all the results across cross section A-A' (Fig. 1).

<sup>b</sup> Campaign 3a and 3b only.

<sup>c</sup> UNSCEAR (2006).

**Table 4**  
Derived dose rate for persons entering the mine.

	Dose rate (μSv h <sup>-1</sup> )				% Tn dose <sup>b</sup>
	Rn ( $DR_{Rn}$ )	Tn ( $DR_{Tn}$ )	Gamma ( $DR_g$ )	Total ( $DR_T$ )	
Mean <sup>a</sup>	0.28	1.22	0.490	1.85	81
UNSCEAR <sup>c</sup>	0.67	1.44	0.490	2.46	68

<sup>a</sup> From Table 3 and Fig. 5.

<sup>b</sup> % Tn dose relates to total inhalation dose only.

<sup>c</sup> Using generic equilibrium factors from UNSCEAR (2006), and mean air kerma, Rn and Tn results from Fig. 5 and Table 3 respectively.

(i.e. in proximity to a work face, or the centre of a work space).

Based on the results and observations from the project it can generally be concluded that:

- thoron may be a major contributor to inhalation dose in historical mines and enclosed areas, and that any monitoring program should be performed after a case-by-case assessment,
- direct monitoring of both radon and thoron progeny is the preferred methodology as equilibrium factors vary considerably between monitoring sites, and within a particular site,
- thoron progeny results appear to be independent of distance from the thoron exhalation surface,
- for the periods monitored in this project, the mean, short term active monitoring results are representative of results obtained from longer term, passive monitoring programs.

#### Ethical statement

Authors state that the research was conducted according to ethical standards.

#### Conflict of interest

Authors state that there is not any conflict of interest.

#### Funding body

This project was partially funded under the Queensland Department of Health, Forensic and Scientific Services Cabinet Research Grant program (grant number RSS15\_008).

#### Acknowledgements

The extensive support provided by Wolfram Camp Mining, including Mick Sturman, Scott Stephens and Darcy Millburn for field support, access to the mine, geological interpretations and 3D mapping

was paramount to the success of the project and is greatly appreciated by the research team. Acknowledgement is also extended to Pushpendra, Kathy and Dimitri from Radiation & Nuclear Sciences, Queensland Department of Health for field, laboratory and logistics support. We would also like to thank Simon Crust, Kingston University, for assisting with provision and reading of intercomparison radon monitors, and NIRS for supplying the thoron progeny monitors for the project.

#### Appendix A. Supplementary data

Supplementary data related to this article can be found at <https://doi.org/10.1016/j.jsm.2018.06.003>.

#### References

- Blevin, P. L. (1989). *The tungsten-molybdenum-bismuth hydrothermal mineralising system at Bamford Hill, northeast Queensland, Australia*. PhD Thesis. Townsville, Australia: Economic Geology Research Centre, James Cook University.
- BOM (2018). *Mareeba airport climate statistics*. Australian Government Bureau of Meteorology. Retrieved 24 Feb, 2018, from [http://www.bom.gov.au/climate/averages/tables/cw\\_031066.shtml](http://www.bom.gov.au/climate/averages/tables/cw_031066.shtml).
- Chen, J., Moir, D., Sorimachi, A., Janik, M., & Tokonami, S. (2012). Determination of thoron equilibrium factor from simultaneous long-term thoron and its progeny measurements. *Radiation Protection Dosimetry*, 149(2), 155–158.
- Cogliano, V. J., Baan, R., Straif, K., Grosse, Y., Lauby-Secretan, B., Ghissassi, E. L., et al. (2011). Preventable exposures associated with human cancers. *Journal of the National Cancer Institute*, 103(24), 1827–1839.
- Darby, S., Whitley, E., Silcocks, P., Thakrar, B., Green, M., Lomas, P., et al. (1998). Risk of lung cancer associated with residential radon exposure in south-west England: A case-control study. *British Journal of Cancer*, 78(3), 394–408.
- Dixon, D. W. (1996). *Exposure to radon during work and leisure activities in caves and abandoned mines*. NRPB Report M667. Chilton: NRPB National Radiological Protection Board.
- FAA. (2017). *FAA's civil aerospace medical Institute radiobiology research team, CARI-7*. United States of America: Federal Aviation Administration. p. Computer Freeware. Retrieved 24 Feb 2018, from: [https://www.faa.gov/data\\_research/research/med\\_humanfacs/aeromedical/radiobiology/cari6/](https://www.faa.gov/data_research/research/med_humanfacs/aeromedical/radiobiology/cari6/).
- Gillmore, G. K., Gharib, H. A., Denman, A. R., Phillips, P. S., & Bridge, D. (2011). Radon concentrations in abandoned mines, Cumbria, UK: Safety implications for industrial archaeologists. *Natural Hazards and Earth System Sciences*, 11, 1311–1318.
- Gillmore, G. K., Phillips, P., Denman, A., Sperrin, M., & Pearce, G. (2001). Radon levels in abandoned metalliferous mines, Devon, Southwest England. *Ecotoxicology and Environmental Safety*, 49(1), 281–292.
- Gillmore, G. K., Sperrin, M., Phillips, P., & Denman, A. (2000a). Radon hazards, geology, and exposure of cave users: A case study and some theoretical perspectives. *Ecotoxicology and Environmental Safety*, 46(3), 279–288.
- Gillmore, G. K., Sperrin, M., Phillips, P., & Denman, A. (2000b). Radon-prone geological formations and implications for cave users. *Technology*, 7(6), 645–655.
- IAEA. (1987). *Preparation and certification of IAEA gamma-ray spectrometry reference materials RGU-1, RGTh-1 and RGK-1*. Report IAEA/RL/148. Vienna: International Atomic Energy Agency. Retrieved 13 Jul 2017, from: [https://inis.iaea.org/search/search.aspx?orig\\_q=RN:18088420](https://inis.iaea.org/search/search.aspx?orig_q=RN:18088420).
- ICRP. (2010). Lung cancer risk from radon and progeny and statement on radon. *ICRP Publication 115*. *Annals of the ICRP*, 40(1), 1–64.
- ICRP. (2014). Radiological protection against radon exposure. *ICRP Publication 126*. *Annals of the ICRP*, 43(3), 5–73.
- ICRP. (2017). Occupational intakes of radionuclides: Part 3. *ICRP Publication 137*. *Annals of the ICRP*, 46(3–4), 1–486. <https://doi.org/10.1177/0146645317734963>.

- Janik, M., Tokonami, S., Kranrod, C., Sorimachi, A., Ishikawa, T., Hosoda, M., et al. (2013). Comparative analysis of radon, thoron and thoron progeny concentration measurements. *Journal of Radiation Research*, 54(4), 597–610. <https://doi.org/10.1093/jrr/rrs129>.
- Kávási, N., Németh, C., Kovács, T., Tokonami, S., Jobbágy, V., Várhegyi, A., et al. (2007). Radon and thoron parallel measurements in Hungary. *Radiation Protection Dosimetry*, 123(2), 250–253.
- Khater, A. E., Hussein, M. A., & Hussein, M. I. (2004). Occupational exposure of phosphate mine workers: Airborne radioactivity measurements and dose assessment. *Journal of Environmental Radioactivity*, 75(1), 47–57.
- Lubin, J. H., & Boice, J. D., Jr. (1997). Lung cancer risk from residential radon: meta-analysis of eight epidemiologic studies. *Journal of the National Cancer Institute*, 89(1), 49–57.
- Malins, A., Machida, M., & Saito, K. (2015). Comment on 'Update of 40K and 226Ra and 232Th series  $\gamma$ -to-dose conversion factors for soil'. *Journal of Environmental Radioactivity*, 144, 179–180. <https://doi.org/10.1016/j.jenvrad.2015.01.009>.
- McLaughlin, J., Murray, M., Currihan, L., Pollard, D., Smith, V., Tokonami, S., et al. (2011). Long-term measurements of thoron, its airborne progeny and radon in 205 dwellings in Ireland. *Radiation Protection Dosimetry*, 145(2–3), 189–193. <https://doi.org/10.1093/rpd/ncr067>.
- Miles, J. C. H., Appleton, J. D., Rees, D. M., Green, B. M. R., Adlam, K. A. M., & Myers, A. H. (2007). *Indicative atlas of radon in England and Wales, HPA-RPD-033*. Chilton: Health Protection Agency.
- Misdaq, M. A., & Ouguidi, J. (2011). Concentrations of radon, thoron and their decay products measured in natural caves and ancient mines by using solid state nuclear track detectors and resulting radiation dose to the members of the public. *Journal of Radioanalytical and Nuclear Chemistry*, 287(1), 135–150.
- Mudd, G. M. (2008). Radon sources and impacts: A review of mining and non-mining issues. *Reviews in Environmental Science and Biotechnology*, 7(4), 325–353.
- Muirhead, C. R., Cox, R., Sather, J. W., MacGibbon, B. H., Edwards, A. A., & Haylock, R. G. E. (1993). Estimates of late radiation risks in the UK population. *Documents of the NRPB*, 4(4), 15–157.
- Ningappa, C., Sannappa, J., Chandrashekar, M. S., & Paramesh, L. (2009). Studies on radon/thoron and their decay products in granite quarries around Bangalore city, India. *Indian Journal of Physics*, 83(8), 1201–1207.
- Nuccetelli, C., & Bochicchio, F. (1998). The thoron issue: Monitoring activities, measuring techniques and dose conversion factors. *Radiation Protection Dosimetry*, 78(1), 59–64. <https://doi.org/10.1093/oxfordjournals.rpd.a032334>.
- Omori, Y., Prasad, G., Sorimachi, A., Sahoo, S. K., Ishikawa, T., Vidya Sagar, D., et al. (2016). Long-term measurements of residential radon, thoron, and thoron progeny concentrations around the Chhatrapur placer deposit, a high background radiation area in Odisha, India. *Journal of Environmental Radioactivity*, 162–163, 371–378. <https://doi.org/10.1016/j.jenvrad.2016.06.009>.
- Przylibski, T. A. (2001). Radon and its daughter products behaviour in the air of an underground tourist route in the former arsenic and gold mine in Złoty Stok (Sudety Mountains, SW Poland). *Journal of Environmental Radioactivity*, 57(2), 87–103.
- Ramola, R. C., Gusain, G. S., Rautela, B. S., Sagar, D. V., Prasad, G., Shahoo, S., et al. (2012). Levels of thoron and progeny in high background radiation area of south-eastern coast of Odisha, India. *Radiation Protection Dosimetry*, 152(1–3), 62–65. <https://doi.org/10.1093/rpd/ncs188>.
- Solli, H. M., Anderson, A., Strandén, E., & Langård, S. (1985). Cancer incidence among workers exposed to radon and thoron daughters at a niobium mine. *Scandinavian Journal of Work, Environment & Health*, 11(1), 7–13.
- Stojanovska, Z., Zunic, Z. S., Bossew, P., Bochicchio, F., Carpentieri, C., Venoso, G., et al. (2014). Results from the integrated measurements of indoor radon, thoron and their decay product concentrations in schools in the Republic of Macedonia. *Radiation Protection Dosimetry*, 162(1–2), 152–156. <https://doi.org/10.1093/rpd/ncu249>.
- Tokonami, S., Takahashi, H., Kobayashi, Y., Zhuo, W., & Hulber, E. (2005). Up-to-date radon-thoron discriminative detector for a large scale survey. *Review of Scientific Instruments*, 76, 3505–3509. <https://doi.org/10.1063/1.2132270>.
- Tschiersch, J., & Meisenberg, O. (2010). The HMGU thoron experimental house: A new tool for exposure assessment. *Radiation Protection Dosimetry*, 141(4), 395–399. <https://doi.org/10.1093/rpd/ncq249>.
- UNSCEAR. (2006). *United nations scientific committee on the effects of atomic radiation UNSCEAR 2006 report to the general assembly*.
- UNSCEAR. (2017). *United nations scientific committee on the effects of atomic radiation UNSCEAR 2017 report to the general assembly*.
- Wheeler, B. W., Allen, J., Depledge, M. H., & Curnow, A. (2012). Radon and skin cancer in south-west england: An ecological study. *Epidemiology*, 23(1), 44–52. <https://doi.org/10.1097/EDE.0b013e31823b6139>.
- WHO. (2018). *Radon and health fact sheet (updated june 2016)*. Retrieved 23 Feb, 2018, from: <http://www.who.int/mediacentre/factsheets/fs291/en/>.
- WHO. (2009). *WHO handbook on indoor radon: A public health perspective*, In H. Zeeb, & F. Shannoun (Eds.). Geneva: World Health Organization.
- Yamada, Y., Sun, Q., Tokonami, S., Akiba, S., Zhuo, W., Hou, C., et al. (2006). Radon-thoron discriminative measurements in Gansu Province, China, and their implication for dose estimates. *Journal of Toxicology and Environmental Health, Part A*, 69(7), 723–734.
- Zhuo, W. H., Iida, T., & Hashiguchi, Y. (2000). Integrating measurements of indoor thoron and its progeny concentrations. *Proceedings of the interantional radiation protection IRPA-10*.
- Zhuo, W., Iida, T., Morizumi, J., Aoyagi, T., & Takahashi, I. (2001). Simulation of the concentrations and distributions of indoor radon and thoron. *Radiation Protection Dosimetry*, 93(4), 357–368.
- Zhuo, T., Tokonami, S., Yonehara, H., & Yamada, Y. (2002). A simple passive monitor for integrating measurements of indoor thoron concentrations. *Review of Scientific Instruments*, 73(8), 2877–2881. <https://doi.org/10.1063/1.1493233>.